Core-Shell Polymerization with Hydrophilic Polymer Cores

Jong Myung Park

Central Research Institute, Kumgang Korea Chemical Co. (KCC), Ltd.,
#85, Mabook-ri, Kuseong-myun, Yongin-si, Kyunggi-do 449-910, Korea

Received November 15, 2000

Abstract : Two-stage emulsion polymerizations of hydrophobic monomers on hydrophilic seed polymer particles were carried out to make core-shell composite particles. It was found that the loci of polymerization in the second stage were the surface layer of the hydrophilic seed latex particles, and that it has resulted in the formation of either eccentric core-shell particles with the core exposed to the aqueous phase or aggregated nonspherical composite particles with the shell attached on the seed surface as many small separated particles. The driving force of these phenomena is related to the gain in free energy of the system in going from the hydrophobic polymer-water interface to hydrophilic polymer-water interface. Thermodynamic analysis of the present polymerization system, which was based on spreading coefficients, supported the likely occurrence of such nonspherical particles due to the combined effects of interfacial free energies and phase separation between the two polymer phases. A hypothetical pathway was proposed to prepare hydrophilic core-hydrophobic shell composite latex particles, which is based on the concept of opposing driving and resistance forces for the phase migration. It was found that the viscosity of the monomer-swollen polymer phase played important role in the formation of particle morphology.

Introduction

The morphology of structured latex particles is of interest because of its relation to particle growth mechanisms in emulsion polymerization and the practical expectation of certain beneficial effects from structured particles. Latex particles of different morphologies usually have been prepared by seeded emulsion polymerization of homogeneous and heterogeneous polymer pairs. It is well-known that, in the semicontinuous emulsion polymerization of monomer II in a seed latex of polymer I, the morphology of the resulting latex particles ranges from homogeneous single domains to an inverted core-shell according to the solubility of monomer II in polymer I, the miscibility between the two polymers, and the hydrophilicity, interfacial tension, and chain flexibility of polymer I.[1-5]

Practical study has been most extensive for the core-shell morphology because such particle morphology affords the improvement of film properties

of the latex. For example, coatings produced from this type of latex display a higher gas and solvent barrier,[6,7] and a higher modulus[8-10] than those produced from homogeneous latex particles of the same composition.

Most of the works mentioned above are limited to the morphology and physical properties of glassy-rubbery polymer pairs with similar hydrophilicity. In the present work, we have taken a glassy-glassy polymer pair with severe hydrophilicity difference (e.g., carboxylated polystyrene and polystyrene) and studied morphology of the resulting composite latex particles. Because the core polymer has a high affinity for water it is difficult to encapsulate well-defined shell around the core in aqueous phase. Therefore, two-stage emulsion polymerizations of this type have been shown to result in a wide variety of particle morphologies including "inverted" core-shell morphology which results from the high hydrophilic nature of the first stage polymer.[11,12] In the present work, we have studied the effect of both thermodynamic and kinetic influences on the morphology of hydrophilic polymer

*e-mail : jmpark@kccworld.co.kr

core/hydrophobic polymer shell composite latex particles under various polymerization conditions. The objectives of this research were to investigate the effect of process parameters on the particle morphology and to search the proper polymerization conditions for the preparation of concentric core-shell polymer particles with hydrophilic polymer cores. One unique application of these composite latex particles is to make hollow polymer particles with an air void as the core, which is obtained by the dewatering of swollen core polymer during drying of the latex. Such particles dispersed in a polymer film would scatter light according to the size of their voids, the refractive index of the polymer and the wavelength of light[13, 14] and thus can be used as an alternative to conventional white pigments for opacifying polymer films.[15, 16]

Experimental

Materials. Reagent grade monomers such as styrene, methacrylic acid, methylmethacrylate, allylmethacrylate and ethyleneglycol dimethacrylate were distilled under reduced pressure and store in a refrigerator. Sodium styrene sulfonate (Dow Chemical Co.), COPS-I (sodium 1-allyl 2-hydroxypropyl sulfonate: Alcolac Chemical Co.) and Span 80 (sorbitan monooleate: ICI America Co.) were used as received. Distilled deionized water (DDI) was used as the continuous phase in all polymerizations. Other chemicals were analytical grade reagents and used without further purification.

Emulsion Polymerization.

Seed Preparation: Batch polymerizations were carried out in both 4-oz capped bottles. For bottle polymerizations, all ingredients except the initiator were added to each bottle. The bottles were sealed with rubber gasketed bottle caps and purged with nitrogen, and then emulsified by hand shaking. The initiator solution was injected using a syringe just before immersed in a preheated water bath. The bottles were tumbled end-over-end at the polymerization temperature for a minimum of 12 hours.

Second Stage Polymerization: Batch and semicontinuous polymerization processes were

used to make the core-shell particles, where the alkali-swellable latices were used as seed. The polymerizations were carried out in 0.5 liter flasks equipped with a reflux condenser, nitrogen inlet, sampling tube, thermometer and stirrer. The flasks were immersed in water bath thermostated at the polymerization temperature. The stirrer speed was maintained at 200 rpm. The polymerizations were carried out under nitrogen atmosphere until completion. In semicontinuous process, the second monomer, styrene, was added continuously to the flask over a certain time period using the Harvard syringe microfeeder. To follow the conversions and the morphological changes of the latex particles taking place during the seeded emulsion polymerization process, aliquots of the latex were taken out at certain time intervals and quenched in ice-water bath with adding small amount of hydroquinone solution to stop further polymerization. Conversions were measured gravimetrically.

Latex Characterization.

Particle Size and Morphology: Transmission electron microscopy (TEM) and photon correlation spectroscopy were used to determine the particle size and size distribution of latices. The latex specimen were prepared by drying dilute samples on a Formvar (polyvinyl formal)-coated TEM grid. Generally, the negative staining by a 2% (w/v) phosphotungstic acid (PTA) aqueous solution was used both for the highly carboxylated latices and for the composite latices comprised of methyl methacrylate or acrylate copolymers in order to prevent deformation of particles during TEM observation. The micrographs obtained using the Philips 300 Transmission Electron Microscope were analyzed using the Zeiss MOP-3 Digital Analyzer. The dispersity of the latex particles was defined by the polydispersity index (U) :

$$U = D_w/D_n$$

Where D_w is the weight-average diameter and D_n is the number average diameter of the particles. The morphology of the composite latex particles were determined using three kinds of electron microscopic methods; latex TEM, scanning electron microscopy (SEM) and shadow casting latex TEM.

52

Korea Polym. J., Vol. 9, No. 1, 2001

Surface and Interfacial Tensions: Surface tensions were measured at room temperature by using duNouy ring method according to ASTM Method D1331. Interfacial tensions were measured by the well-known drop-volume technique using Gilmont micrometer syringe connected to the glass capillary of accurately known outer diameter. Drops were formed quickly to 90% of their final volume, then kept at rest for a few minutes to ensure interface equilibrium and finally increased slowly in size until they detached from the capillary. The drop volume of the aqueous solution was measured five times for each sample. Interfacial tension values were calculated by using the correction factors established by Lando and Oakley.[17]

Results and Discussion

Preparation of Highly Carboxylated Polymer Seed Latices. Standard polymerization recipe for the alkali-swellable seed latices is given in Table I. A small amount of ionogenic functional monomers such as NaSS and COPS-I was employed to overcome the latex instability often

Table I. Standard Recipe Used to Prepare 70/30 (wt) Styrene-Methacrylic Acid Copolymer Seed Latices

Ingredients	Weight(gm)
Styrene	7
Methacrylic acid	3
Ethyleneglycol dimethacrylate	0.1
NaSS	Variable[a]
Potassium persulfate	Variable[b]
DDI water	56

[a]5 levels of [NaSS]; 0.02, 0.04, 0.07, 0.15 and 0.2.
[b]2 levels of [KPS]; 0.04 (L-series) and 0.12 (H-series).

encountered in emulsifier-free polymerizations. Methacrylic acid was chosen as the acid functional monomer to make the latex particles alkali-swellable because its distribution between the aqueous and monomer/polymer phases favors the latter to a greater extent than acrylic acid, even though its distribution within the particles is not uniform.[18,19] Ethyleneglycol dimethacrylate (EGDMA) was used as the crosslinking monomer to regulate the swellability and morphology of the final composite latices; its incorporation prevents non-uniform swelling of the core particles and migration of the hydrophilic chain segment to the particle surface during the subsequent core-shell polymerization stage.[20] The optimum amount of EGDMA was found to be around 1 wt% based on the monomers. As shown in Table I, two levels of initiator (potassium persulfate), designated as L (low) and H (high) series, and five levels of sodium styrene sulfonate (NaSS) were used to control the diameter of seed latex particles. The particle diameter results were summarized in Table II. It is clearly shown that the particle diameter is strongly dependent upon the NaSS concentration, but weakly dependent upon the initiator concentration. Generally, as the concentration of functional monomer is increased, the particle size decreases,[21] but as the concentration of initiator is increased, the particle size either increases due to the increase of ionic strength or decreases due to the increased free radical concentration. These generalizations apply mainly to systems with little or no emulsifier where the particles flocculate and coalesce until the latex particles become stable,[22] as is the case of the present system. Therefore, the stability of the latices is an important factor which controls particle size. Particle size was decreased with the increasing initiator concentration at high concentration of NaSS where effect of number of

Table II. Particle Size of L and H Series Seed Latices

	Latex Sample Number				
[KPS][a]	1	2	3	4	5
[NaSS][a]	0.2	0.4	0.7	1.5	2.0
	Particle Diameter (D_n) (nm)				
0.4 (L1 to L5)	130	111	95	82	71
1.2 (H1 to H5)	140	121	94	85	66

[a]Concentrations are in weight percent, based on monomers.

Korea Polym. J., Vol. 9, No. 1, 2001

53

radicals was dominant, but it was increased at low concentration of NaSS where ionic strength effect was dominant.

Seeded Emulsion Polymerization.

Effect of Size of Seed Latex: Batch seeded emulsion polymerizations were carried out at 60 °C using L- and H-series seed latices using the recipe given in Table III to investigate the effect of seed latex on the morphology of the composite latices. The conversion-time curves for seeded emulsion polymerizations (CS-L series) using L-series seed latices are shown in Figure 1. The number next to CS-L designation indicates the seed latex number given in Table II, which was used in the seeded polymerization. The initial rate of the seeded polymerization is shown in Figure 1 to increase with increasing NaSS concentration used in the preparation of the seed latex. This may be due in part to increases in the surface area of the seed particles. Figure 2 shows the relationship between the initial polymerization rate and the particle diameter of the seed. In the lower range of the seed size (71-95 nm), the rate of polymerization is proportional to the 0.7 power of the diameter of the seed latices and for the upper range of seed size (111-130 nm) to the 5.5 power of the diameter of the seed latices. There seems to be a transition between the two ranges. The parti-
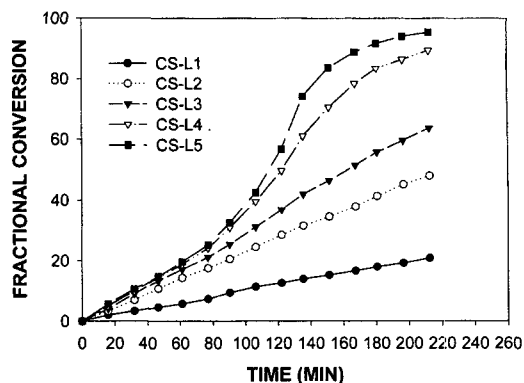

Figure 1. Conversion-time curves of seeded polymerization of styrene using styrene-based seeds (S-L series).
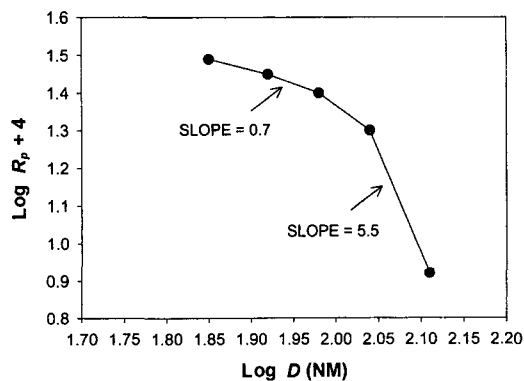

Figure 2. Dependence of the rate of polymerization on the size of the seed particles.

cle diameters and shape of the CS-L series composite latices are summarized in Table IV. All composite latices except CS-L1 have a pear-shaped morphology. The effect of seed size on the morphology of composite latices was reported by Yamazaki et al.,[23] where they have investigated methods of obtaining emulsifier-free latices of composite polymers in which the particles have a two-layered structure through seeded polymeriza-

Table III. Standard Recipe used to Prepare Two-Stage Composite Latices

Ingredients	Weight(gm)
Seed latex (15% solid)	40.00
Styrene	60.00
Sodium styrene sulfonate (NaSS)	0.12
Potassium persulfate (KPS)	0.24
DDI water	230.00

Table IV. Particle Diameter and Shape of CS-L Series[a]

	D_n (nm)	PSD	D_n (theo)[b]	Shape
CS-L1	251	1.04	249	Spherical/dumbbell
CS-L2	218	1.03	210	Pear-shaped
CS-L3	190	1.01	182	Pear-shaped
CS-L4	157	1.01	156	Pear-shaped
CS-L5	137	1.03	142	Pear-shaped

[a]Batch seeded polymerization at 60 °C in a tumbler reactor with stage ratio of 6.

[b]Theoretical D_n was calculated on the assumption of no new crops of secondary particles.

54

Korea Polym. J., Vol. 9, No. 1, 2001

tion of methyl methacrylate on polystyrene and styrene on polymethylmethacrylate seed particles. Under the synthetic conditions they used, stable monodisperse latices could be formed if the diameter of the seed particles did not exceed 200 nm. Dimonie et al.[24] also reported similar results in the seeded emulsion polymerization of a styrene-acrylonitrile comonomer mixture in polystyrene seed latices. They obtained the copolymer latices having core-shell morphology only when the level of seed surface area was larger than certain value, which was more easily achieved with the smaller seed particles. In both cases, the importance of the seed size on both morphology and polymerization kinetics was shown, as is the case in the present study.

Batch seeded polymerizations using the H-series seed latices, however, resulted different kinetic behavior compared to the CS-L series. There was no dependence of the initial polymerization rate on the surface area of the seed particles. In this case the stability of the seed latices may play a more important role on rate of polymerization and thus the rate of polymerization was dependent on the number of final latex particles, which was mainly determined by the ionic strength of the system. In addition to the irregular kinetic behavior it was found that the particle morphologies of CS-H series composite latices were different from CS-L series composite latices. CS-H composite latices were comprised of mixture of spherical and pear-shaped particles with a bimodal size distribution. From the investigation of the particle growth using TEM for latex samples taken during the second stage of polymerization, it was found that most second stage monomer formed new crops of polymer particles and grew as spherical particles. These results indicated that the loci of polymerization for the CS-H series were not surface area of seed particles but individual particles generated during the second stage polymerization. It should be however noted here that the effect of initiator concentration used in seed preparation affects the behavior of particle growth significantly only in highly carboxylated seed systems. For instance, there is little effect of initiator concentration over the range studied on the particle morphology in the 80:20 styrene-methacrylic acid seed latex

system.

Effect of Degree of Monomer Starvation. Three different modes of styrene monomer addition were used to evaluate the effect of monomer starvation on the particle morphology for these seeded emulsion polymerizations. They are : (1) batch process (all monomer added at the beginning of the polymerization), (2) a semicontinuous process with a fast monomer feeding rate of 0.75 cc/min, and (3) a semicontinuous process with a slow monomer feeding rate of 0.15 cc/min. L4 latex was used as the seed in this study. The conversion-time curves of these seeded polymerizations are shown in Figure 3. It can be seen that the rate of polymerization is dependent on the degree of monomer starvation; the maximum rate is achieved for the batch seeded polymerization. For the monomer-starved run, the rate of polymerization is parallel to the monomer addition rate for most of the polymerization period and drops off after the monomer addition is completed. The electron micrographs in Figure 4 show an interesting trend in the evolution of particle morphology during this polymerization. The arrows on the curves in Figure 3 correspond to the micrographs in Figure 4. The particle growth in monomer-starved semicontinuous polymerization is similar to that in batch polymerization with respect to localization of shell polymers on the surface of seed particles. However, the number of loci is greater in the monomer starved process than in
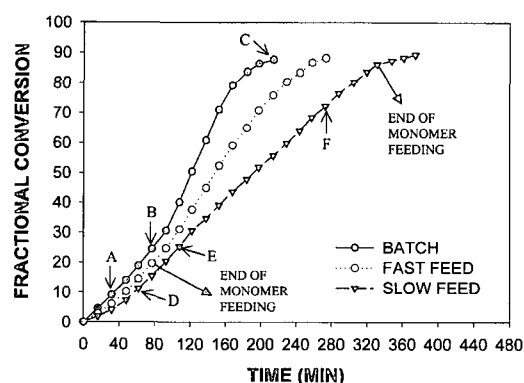

Figure 3. Conversion-time curves of seeded polymerization using different modes of monomer addition : (A) batch process, (B) semicontinuous process with fast feeding, and (C) semicontinuous process with slow feeding.
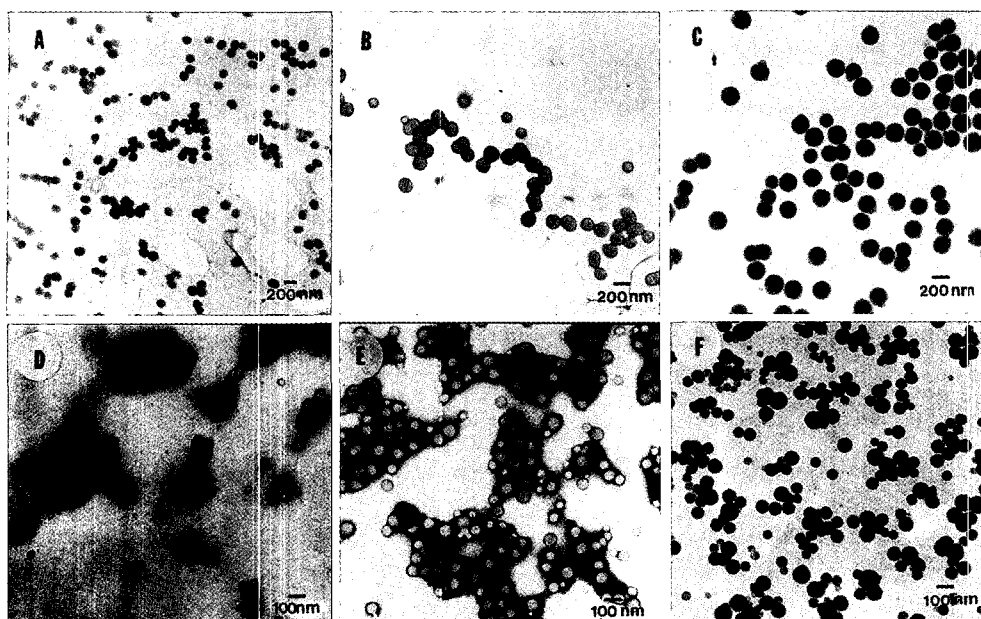
Figure 4. TEM micrographs of poly(styrene-co-methacrylic acid)-polystyrene composite particles (Figure 3) at various conversions : (A) 19.0%, (B) 36.7%, (C) 75.0%, (D) 18.8%, (E) 29.9%, and (F) 96.8%.

batch process. This is due to the effect of viscosity of polymerization loci on the particle growth. The monomer to polymer ratio (M/P) at a given conversion is much lower in monomer-starved run than that in monomer-flooded run. For instance, the monomer to polymer ratio at the point B in Figure 3 is 0.15 for the semicontinuous polymerization compared to 1.75 for the batch polymerization. These results and other observations suggest that the particle growth mechanism in a seeded polymerization using more hydrophilic seed particles compared to the second stage monomer follows the scheme given in Figure 5. The primary particles of the second-stage monomer may be formed in the aqueous phase and heterocoagulate with the hydrophilic seed particles. The driving force of such heterocoagulation seems to be the instability of primary particles formed at the given concentration of NaSS. The primary particles tend to be deposited onto the more hydrophilic seed particles to gain their colloidal stability. As a result of interfacial tension, the hydrophobic monomer-swollen particles tend to contract and form a minimum surface area, so that the shell polymer forms the other spherical contour. The degree of contraction depends on
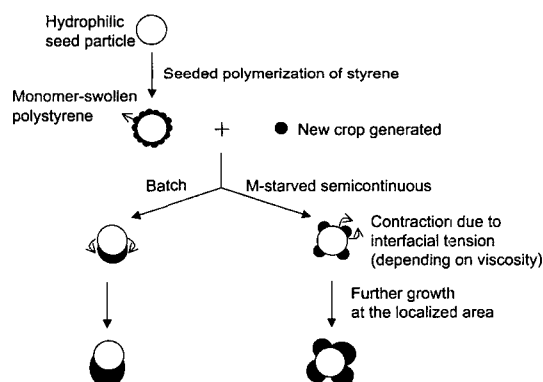

Figure 5. Particle growth mechanism of the composite latices.

the viscosity of the monomer-swollen shell polymers. In the case of the monomer-starved polymerization, the viscosity of the loci is quite high and hence limits the degree of contraction. Figure 4(A) provides clear evidence of this behavior. On the other hand, the lower viscosity of the monomer-swollen shell polymer in batch polymerization cannot limit the degree of contraction and hence results in an ellipsoidal shape as shown in Figure 4(D). Further growth of the localized shell region

56

results in dumbbell-shaped particles in batch polymerization and popcorn shaped particles in monomer-starved semicontinuous polymerization, which is seen in Figure 4(B) and 4(E), respectively. In the case of high stage ratio, as is the case of this study, more further growth results in pear-shaped morphology in batch polymerization, as shown in Figure 4(F). On the other hand, further growth of the distinctly spherical shell polymer region in monomer-starved polymerization finally leads to the rupture of popcorn-shaped composite particles into bunches of small particles, as shown in Figure 4(C). Because of the complete incompatibility the adhesion between the two is physical rather than chemical or chain-entangled. Thus, when the diameter of the shell spheres adhering to the seed particles exceeds a certain limit, the particles are apt to be disintegrated by hydrodynamic forces. The sudden increase of latex viscosity at the end of the polymerization supports the occurrence of the particle disintegration.

MMA-Based Seed System. The particle growth was also studied in two-stage emulsion polymerizations using 70:30 methyl methacrylate-methacrylic acid copolymer latex as the seed and styrene as the second-stage monomer. The seed latices were synthesized according to the recipe given in Table II except for the kind of main monomer. The polymerization conditions of the

seeded polymerizations were the same as that of Table III except for the kind of seed latices. In batch polymerization, an evolution of particle growth could not be followed over the whole polymerization period because the latex became gel-like at a low conversion of about 21%. Particle growth behavior similar to that seen in Figure 4 was also found in MMA-based seed system. In the monomer-starved semicontinuous polymerization, the number of lumps on the seed particles was greater than in the monomer-flooded polymerization, as shown in Figures 6(A) and 6(E), respectively. Comparing the particle morphology of MMA-based seed system with that of styrene-based seed system, the number of lumps was almost threefold greater in the former case. This may reflect the difference in affinity between the seed and shell polymers, i.e., the MMA-MAA copolymer shows stronger affinity to polystyrene shell polymer than the styrene-MAA copolymer does. This is due in part to the strong van der Waals attraction induced by the polarity difference. In order to achieve a core-shell morphology, the localization of polymerization site on a part of seed surface should be minimized. The present study shows that this localization was lesser in the semicontinuous polymerization than in the batch polymerization, and lesser in the MMA-based seed system than in the styrene-based seed sys-
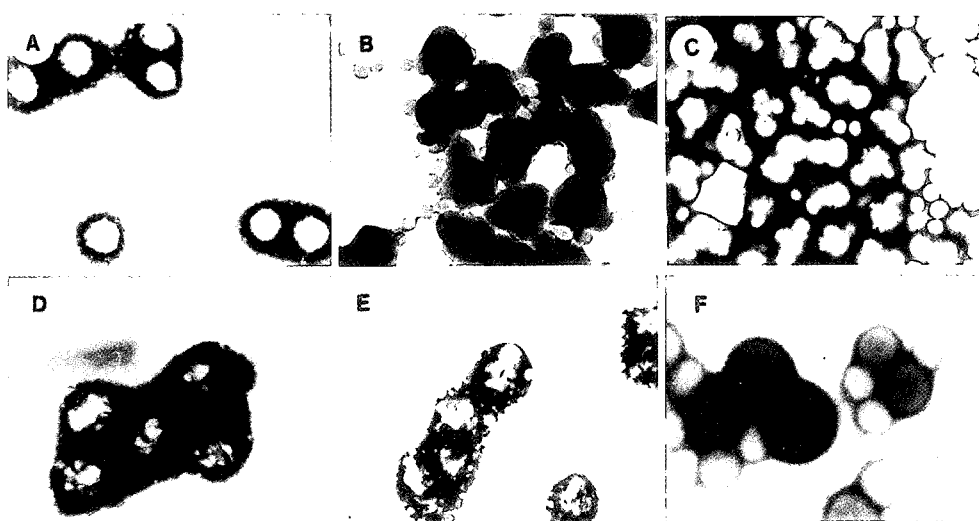

Figure 6. TEM micrographs of poly(methyl methacrylate-co-methacrylic acid)-polystyrene composite particles at various conversions : (A) 17.2%, (B) 26.5%, (C) 94.2%, (D) 13.2%, (E) 18.7%, and (F) 21.5%.

tem.

Thermodynamic Consideration. As presented in the previous sections, batch seeded emulsion polymerization of styrene on highly carboxylated polystyrene particles gave eccentric core-shell particles with the core exposed to the aqueous phase; semicontinuous polymerization gave aggregated nonspherical particles with well-defined polystyrene and carboxylated polystyrene regions. In contrast, the batch seeded emulsion polymerization of styrene on highly carboxylated polymethylmethacrylate particles gave aggregated nonspherical particles; semicontinuous polymerization gave confetti-like particles. The driving force of these phenomena is related to the gain in free energy of the system in going from the hydrophobic polymer-water interface to hydrophilic polymer-water interface. Also, the high viscosity of the monomer-swollen polymer particles, which in semicontinuous polymerization is controlled by the rate of monomer addition, acts to reduce the contraction of the polymer shell and leads to the formation of composite particles, each of which has several lumps on their surface. These results well illustrate the importance of thermodynamic influence as well as kinetic characteristics for the development of particle morphology. In this section, a thermodynamic analysis of the system was provided to redesign the polymerization condition for the preparation of concentric core-shell particles.

Figure 7 depicts the beginning of the seeded emulsion polymerization, in which the three components --- water (w), monomer-swollen polymer (p), seed surface (s) --- interact with each other. Thus there are three different interfacial tensions --- γ_{pw}, γ_{sw} and γ_{sp}. The resulting equilibrium configuration of the three phases in contact can be predicted from the interfacial tensions and spreading coefficients. For simplicity, it was assumed that only one spreading coefficient S_p is operative and that the effects of the physical and chemical heterogeneities and the curvature of the seed particle surface can be neglected. Thus the system is considered as the process of wetting of solid (s) by liquid (p) in the water phase (w), which can be described in terms of interfacial tensions by Young's equation. This system has two limiting configurations: 1. a concentric core-shell
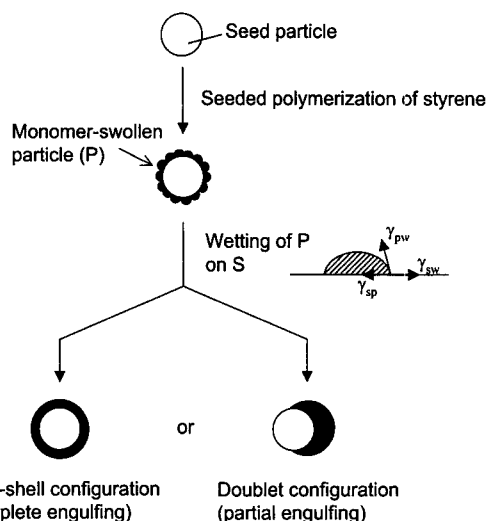

Figure 7. Representation of the seeded polymerization of styrene onto seed particles resulting in the formation of core-shell or doublet configuration morphologies.

(complete engulfment); 2. a doublet of the two polymers (partial engulfment). The core-shell configuration is likely to result when the spreading coefficient S_p is positive, and the doublet configuration when it is negative.

For the core-shell configuration,

$$\gamma_{sw} > (\gamma_{sp} + \gamma_{pw})$$

and for the doublet configuration,

$$\gamma_{sw} < (\gamma_{sp} + \gamma_{pw}).$$

Thus the core-shell morphology is favored by increasing γ_{sw}, decreasing γ_{sp}, and decreasing γ_{pw}.

This simple analysis based on Young's equation was extended to the general case in which all three spreading coefficients --- S_s, S_w, S_p. --- are operative. The general case[25] assumes that the two immiscible liquids 1 and 3 are suspended in the immiscible liquid 2. From the general expression for the spreading coefficients,

$$S_i = \gamma_{jk} - (\gamma_{ij} + \gamma_{ik}),$$

there are four sets of values (the set $S_1 < 0$, $S_2 > 0$, $S_3 > 0$ is algebraically impossible):

$S_1 < 0, S_2 < 0, S_3 < 0$

$S_1 < 0, S_2 < 0, S_3 > 0$

$S_1 < 0, S_2 > 0, S_3 < 0$

$S_1 > 0, S_2 < 0, S_3 < 0.$

These four sets of values correspond to the four different equilibrium configurations shown in Figure 8: 1. core-shell (complete engulfment); 2. doublet (partial engulfment); 3. individual separated particles (non-engulfment); 4. inverse core-shell (inverse engulfment). This analysis assumed that there is no permutation of phases, i.e., component 2 is always the continuous phase. Let us now apply this general treatment to the present case, in which one component is solid (seed particle) instead of liquid, using the original nomenclature to avoid confusion: component 1 = seed surface (s); component 2 = water (w); component 3 = monomer-swollen polymer (p). The first three configurations of Figure 8 is still the same, but the fourth configuration is now nonexistent. The four
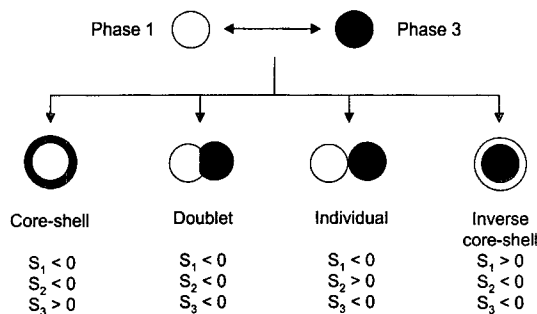

Figure 8. Generalized representation for possible equilibrium configurations predicted using spreading coefficients. In this case Phase 1 and Phase 3 are liquids.
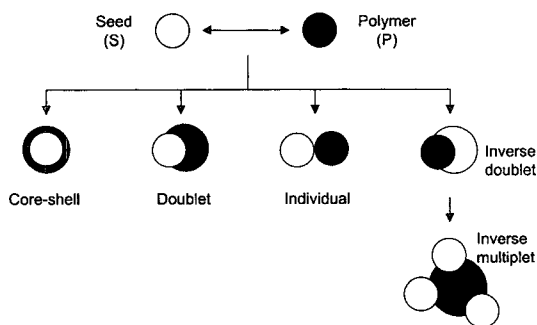

Figure 9. Representation of possible composite latex morphologies predicted using spreading coefficients. In this case Phase 1 is a seed latex and Phase 3 is monomer-swollen polymer.

corresponding configurations are depicted in Figure 9.

Thus, for the core-shell configuration,

$S_s = \gamma_{pw} - (\gamma_{sp} + \gamma_{sw}) < 0$

$S_w = \gamma_{sp} - (\gamma_{sw} + \gamma_{pw}) < 0$

$S_p = \gamma_{sw} - (\gamma_{sp} + \gamma_{pw}) > 0$

for the doublet configuration,

$S_s = \gamma_{pw} - (\gamma_{sp} + \gamma_{sw}) < 0$

$S_w = \gamma_{sp} - (\gamma_{sw} + \gamma_{pw}) < 0$

$S_p = \gamma_{sw} - (\gamma_{sp} + \gamma_{pw}) < 0$

for the configuration of two individual separated particles,

$S_s = \gamma_{pw} - (\gamma_{sp} + \gamma_{sw}) < 0$

$S_w = \gamma_{sp} - (\gamma_{sw} + \gamma_{pw}) > 0$

$S_p = \gamma_{sw} - (\gamma_{sp} + \gamma_{pw}) < 0$

and for the inverse doublet configuration,

$S_s = \gamma_{pw} - (\gamma_{sp} + \gamma_{sw}) > 0$

$S_w = \gamma_{sp} - (\gamma_{sw} + \gamma_{pw}) < 0$

$S_p = \gamma_{sw} - (\gamma_{sp} + \gamma_{pw}) < 0$

Another approach to obtain similar criteria was based on the free energy changes of the system, which was originally suggested by Sundberg et al.[26] An approximate thermodynamic analysis of the present system was developed by taking into account the free energy changes taking place in a hypothetical pathway. The initial state is that of the seed particles and the monomer swollen polymer phase dispersed separately in the water phase. The final state is one of the morphologies shown in Figure 9. If it is assumed that there are no phase changes or mixing or demixing, the only contribution to the free energy change is that of the creation of new interfaces. The final equilibrium state of three phases will therefore be that which has a minimum surface free energy. Therefore, the reduced free energy, which was defined as the free energy change per unit surface area of the particles, for the core-shell configuration of Figure 9 is

$$(\gamma_{sp} - \gamma_{sw}) \ (M/P + 1)^{-2/3} + \gamma_{pw}$$

and for the configuration of two individual particles

$$\gamma_{pw} \ (M/P + 1)^{-2/3} (M/P)^{2/3}$$

where M/P is the monomer to polymer weight ratio.

The reduced free energy changes for the doublet or inverse doublet configuration are dependent on the degree of engulfing and M/P ratio. Therefore, it ranges from that of eccentric core-shell configuration for most engulfing to that of two individual particles for least engulfing.

This analysis showed that the most probable configuration was determined by the interfacial tensions and the M/P ratio. However, it should be noted that the effect of M/P ratio is not as important as that of the interfacial tensions for the development of particle morphology especially for monomer-starved semicontinuous process, because the final morphology is usually determined during early stage of polymerization where M/P ratio is near zero. It is true even in batch process when the partitioning of second stage monomer to seed particle is low, as is the case in this research. As M/P ratio approaching zero, then the reduced free energy change for the core-shell configuration becomes

$$\gamma_{sw} - (\gamma_{sp} + \gamma_{pw})$$

which is the single spreading coefficient criterion (S_p). For the other configurations including the doublet configuration, it becomes zero. S_p should be negative for the core-shell configuration. Therefore, thermodynamic consideration based on the spreading coefficients was used to predict the most probable configuration in this work. Table V shows the configurations predicted for selected sets of interfacial tension values. System 1 represents an actual polymerization system comprised of hydrophilic seed particles, water and styrene monomer. The polymer-water interfacial tension was estimated to be ca. 30 dynes/cm from the measurements of the interfacial tension between 0.1% polystyrene solution in styrene and water shown in Table VI. The polymer-water and seed-polymer interfacial tensions were estimated to be ca. 2 and 10 dynes/cm, respectively. The values of spreading coefficients calculated from these interfacial tensions predicted the formation of nonspherical particles, which was in accord with the experimental results shown in the previous section.

The effect of surfactant dissolved in the monomer phase on the particle morphology (System 3) was also examined. Span 80 emulsifier (soluble in styrene; insoluble in water) added to the styrene

Table VI. Interfacial Tension by Drop Volume Method

Oil phase	γ_{pw} (dyne/cm)
Styrene	43
Styrene + Polystyrene[a]	25.6
Styrene + Span 80[b] (10^{-4} mole%)	27.2
Styrene + Span 80 (3×10^{-4} mole%)	15.3
Styrene + Span 80 (10^{-3} mole%)	8.1
Styrene + Span 80 (2×10^{-3} mole%)	8.3

[a] 0.1 wt% polystyrene (Dow polystyrene latex purified).
[b] Span 80; sorbitan monooleate, HLB 4.3.

Table V. Prediction of Equilibrium Configuration from Spreading Coefficients

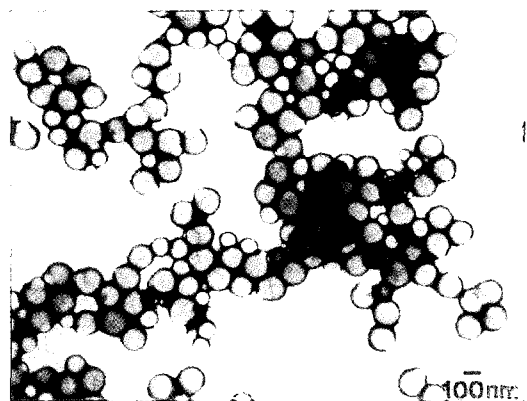| System	γ_{sw}	γ_{sp}	γ_{pw}	S_s	S_w	S_p	Probable Configuration
1	2	10	30	18	-22	-38	inverse
2	2	5	10	3	-7	-13	inverse
3	2	2	2	-2	-2	-2	doublet
4	10	5	15	0	-20	-10	doublet
5	10	5	5	-10	-10	0	core-shell
6	20	5	30	5	-45	-15	inverse
7	20	10	10	-20	-20	0	core-shell
8	20	5	10	-15	-25	5	core-shell

60

Korea Polym. J., Vol. 9, No. 1, 2001

Figure 10. TEM micrograph of two-stage composite latex prepared by batch polymerization at 60 °C with 10^{-3} moles Span 80 in the styrene monomer.

phase decreased the styrene-water interfacial tension significantly (Table VI). Table V shows that the formation of nonspherical particles was predicted for this System 3, which was in accord with the shape of particles shown in Figure 10. The polymerization conditions used to prepare these particles were the same as those given in Table II except for the addition of the Span 80 into the second stage monomer. The morphology of the final composite particles was the same as that of latices produced without addition of Span 80 except that more new particles were generated. This implies that the decrease of interfacial tension between polymer and water alone is not enough for the control of particle morphology. In addition to the decreasing of γ_{pw}, γ_{sw} should be increased and γ_{sp} should be decreased in order to obtain core-shell morphology (Systems 5, 7, 8 of Table V).

Resistance to Phase Migration. These predictions provide only a qualitative guide to the effect of interfacial tension and M/P ratio on the morphology of the composite particles. The real systems are much more complex because of the chemical and physical changes that occur during the development of the particle morphology; nevertheless, the final equilibrium state is determined by the interfacial tensions and M/P ratios, which suggests that gravity, fluid flow, and interparticle forces do not determine the position of the equilibrium but may affect the rate of its attainment. The main concept of this study is the consider-

ation of the interfacial tension as the driving force and the following factors as resistance forces. These resistance forces include: 1. viscosity or polymer chain mobility; 2. degree of interpenetration (physical entanglement of polymer chains) of the second-stage and seed polymers; 3. chemical binding of the two polymer phases; 4. special interactions such as acid-base interactions.

The effect of viscosity of the monomer-swollen polymer particles on the particle morphology was studied by Matsumoto et al.,[27-30] who determined the morphology of composite latices prepared by batch or semicontinuous polymerization of styrene in polyethylacrylate or polymethylmethacrylate seed latices; the number of polystyrene domains in the polyethylacrylate seed particles was 4-5 fold greater in the latices prepared by semicontinuous polymerization than in those prepared by batch polymerization. Similar results were found in this research; the number of polystyrene domains in the 70 : 30 styrene-methacrylic acid copolymer particles was 4-fold greater in the latices prepared by semicontinuous polymerization than in those prepared by batch polymerization. These results confirm the important role of the viscosity of the monomer-swollen particles in determining the morphology of particles comprising incompatible polymer pairs.

In addition to the mode of polymerization, the polymerization temperature and the rate of radical generation also influence the viscosity of the monomer-swollen particles, e.g., the number of polystyrene domains in the 70 : 30 styrene-methacrylic acid copolymer seed particles prepared by batch polymerization at 50 °C was 3-4 fold greater using potassium persulfate-sodium bisulfite redox initiator (Figure 11(A)) than using potassium persulfate alone (Figure 11(B)). The higher rate of radical generation gave a higher viscosity of the monomer-swollen particles, which resulted in more polystyrene inclusions.

Allyl methacrylate was incorporated into the seed latex particles to promote interfacial adhesion by grafting. The so-called "shot-growth" method[30] was used to incorporate grafting sites (residual double bonds) in the seed latex particle surface. The allyl methacrylate was added to the polymerization at 82% conversion, and the poly-
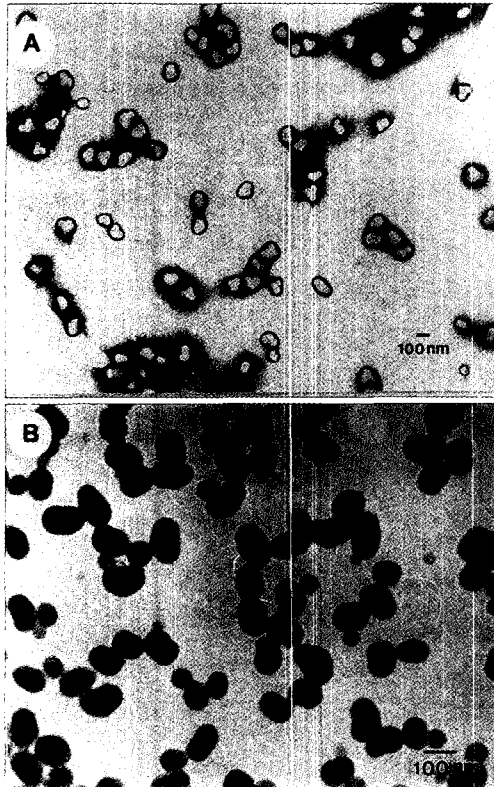
Figure 11. TEM micrographs of two-stage composite latices prepared by batch polymerization at 60 °C using: (A) potassium persulfate-sodium bisulfite redox initiator and (B) potassium persulfate initiator.

merization was carried out to completion. Figure 12(A) shows the morphology of the seed particles. Styrene was polymerized in the seed particles at 60 °C using both batch and semicontinuous polymerization. Figures 13(B) and 13(C) show the morphologies of the particle prepared by batch and semicontinuous polymerization, respectively. There were 2-3 polystyrene domains in the particles prepared by batch polymerization and 7-8 domains in those prepared by semicontinuous polymerization; the corresponding numbers of polystyrene domains in the particles prepared without allyl methacrylate were 1 and 3, respectively, which shows that the incorporation of allyl-methacrylate promoted the interfacial adhesion by furnishing grafting sites, especially in semicontinuous polymerization, but it was not enough to get concentric core-shell particles.

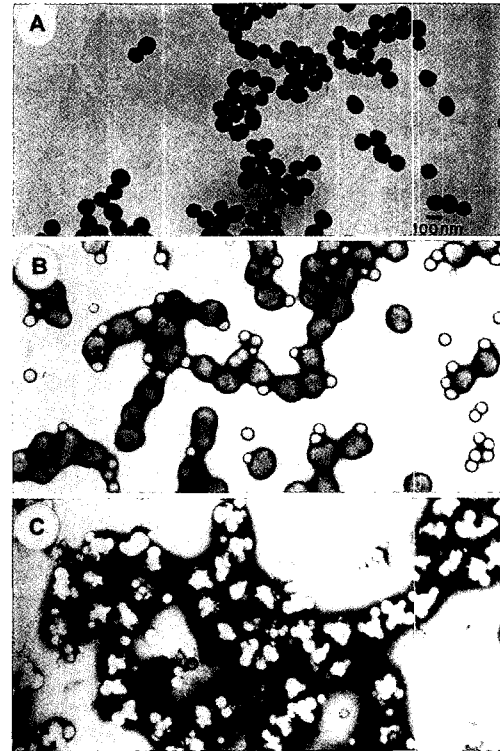The higher initiator concentration may enhance

Figure 12. TEM micrographs of two-stage composite latices: (A) seed latex containing allyl methacrylate, (B) final latex prepared by batch polymerization, and (C) final latex prepared by semicontinuous polymerization.
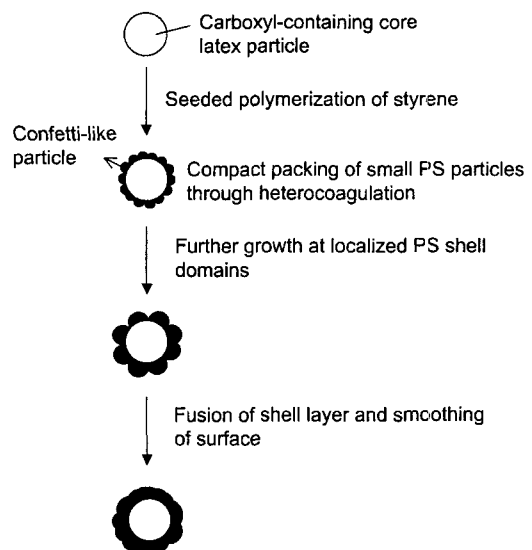

Figure 13. Hypothetical pathway proposed to prepared hydrophilic core and hydrophobic shell composite latex particles.

62

Korea Polym. J., Vol. 9, No. 1, 2001

the encapsulation of the hydrophilic core with a hydrophobic shell because of the anchoring effect of ionic end groups of the polymer chains. This is also attributed in part to the lower interfacial tension between the polymer shell and the water phase (γ_{pw}) resulting from the higher surface charge density as shown in Table VI. Cho and Lee[5] demonstrated that a core-shell morphology of a polystyrene shell around a polymethylmethacrylate core was attainable at high concentration of persulfate initiator. However, it was found in this work that the particle morphology was independent on the kind of initiator, in other words, eccentric core-shell particles were obtained regardless of using water-soluble initiator (KPS) or oil-soluble initiator (AIBN). This implies that the anchoring effect of the ionic chain ends is applicable only for the small hydrophilicity difference between core and shell polymers.

Particle Growth Mechanism of Core-Shell Particles. It has been demonstrated in the previous sections that two stage emulsion polymerizations of hydrophobic monomers onto hydrophilic seed polymer particles have resulted in the formation of either eccentric core-shell particles with the core exposed to the aqueous phase or aggregated nonspherical composite particles with the shell attached on the seed surface as several small separated particles. Thermodynamic analysis of the present polymerization system supported the formation of such nonspherical particles rather than concentric spherical core-shell particles because of the combined effects of interfacial free energies and phase separation between the two polymer phases. In addition, it was shown experimentally that the composition of the seed latices and the viscosity of the monomer-swollen polymer phase played important roles in the formation of particle morphology. One of the promising ways to prepare latices with concentric core-shell morphologies was proposed in Figure 13, which is based on the heterocoagulation mechanism. The idea involved in the postulation of such a hypothetical pathway is the consideration of the interfacial tension as the thermodynamic driving force for phase migration and the viscosity as the kinetic resistance to this migration. Thus, the important points are as follows:

1. In emulsifier-free emulsion polymerization, the secondary particles formed in the aqueous phase may carry less monomer compared to those in conventional emulsion polymerization. This may happen because there is no emulsifier in the aqueous phase for nucleation in micelles.

2. The higher viscosity of the monomer-swollen polymer phase shell therefore results when the secondary particles formed in the aqueous phase heterocoagulate onto the seed particle surfaces.

3. The partitioning of the second stage monomer in the seed latices should be as low as possible to achieve a lower monomer/polymer ratio in the polymer shell layer. This suggests that the methylmethacylate-based seed latices may be better than styrene-based seed latices for the seeded polymerization of styrene.

4. The high instantaneous conversion during the second stage may help to increase the viscosity of the shell layer. This is controlled by decreasing the rate of monomer addition along with the initiator concentration.

5. The higher viscosity of the shell layer works against its contraction to form eccentric core-shell particles.

The proposed growth mechanism was experimentally confirmed by using well designed polymerization conditions[31] so as to follow the hypothetical pathway. Figure 14 shows the evolution of particle morphologies during the second stage emulsion polymerization. It was clearly shown that growth pattern of the composite latices closely resembled that of the hypothetical pathway given in Figure 13. During the second stage of polymerization, i.e., the seeded polymerization of styrene in the presence of acid-containing core particles, most of the monomer initially polymerized in the aqueous phase and subsequently homocoagulated as secondary particles, which then heterocoagulated on the more hydrophilic seed surface to enhance stability as shown in Figure 14(B), because there was not enough surfactant present in the system and because the partitioning of styrene into the seed copolymer was probably very low. Heterocoagulation of polystyrene particles on the seed particles was followed by the further polymerization of styrene in those localized domains, as shown in Figure 4(C). The uneven surfaces of
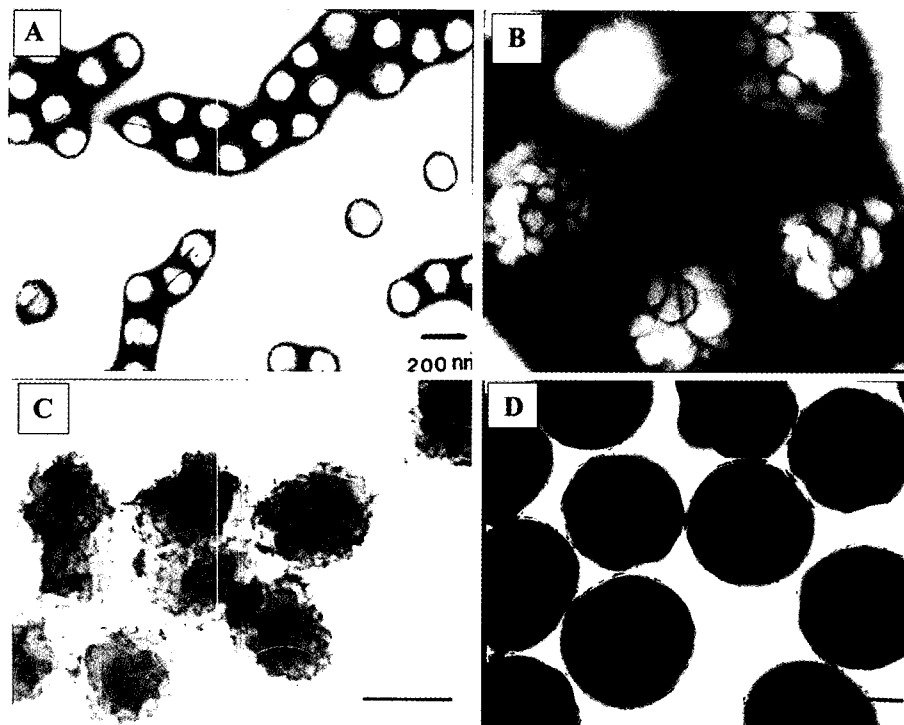
Figure 14. TEM micrographs showing the evolution of the particle morphologies under the redesigned polymerization conditions: (A) seed latex, (B) at 16%, (C) at 26% and, (D) at 96% conversion of the second stage of polymerization.

most of the larger composite particles also reflect such a unique pattern of particle growth, as shown in Figure 14(D), and show the occurrence to some degree of the fusion of the shell layer to give a smooth surface, even though the polymerization conditions such as the monomer feed rate and the monomer/polymer ratio were not sufficient to give completely smooth surfaces.

Conclusions

The following conclusions were derived from this study of the two-stage emulsifier-free polymerization of styrene in the presence of carboxylated polystyrene or poly(methyl methacrylate) latices:

The use of ionogenic comomomers such as sodium styrene sulfonate and sodium 1-allyloxy-2-hydroxypropyl sulfonate allowed the control of the latex particle size as well as the colloidal stability; however, high concentrations gave a new crop of small latex particles because of the formation of water-soluble polymers.

The particle growth of the seed copolymer latex followed the general emulsifier-free emulsion polymerization mechanism, which indicates that the colloidal stability played an important role during particle nucleation and growth.

The batch seeded emulsion polymerization of styrene onto highly carboxylated polystyrene particles gave eccentric core-shell particles with the core exposed to the aqueous phase, while semi-continuous seeded polymerization gave aggregated nonspherical particles with well-defined polystyrene and carboxylated polystyrene regions.

The batch seeded emulsion polymerization of styrene onto highly carboxylated poly(methyl methacrylate) particles gave aggregated particles, while semicontinuous seeded polymerization gave confetti-like particles. The driving force of these phenomena is related to the decrease of free energy of the system in going from the hydrophobic polymer-water interface to the hydrophilic polymer-water interface. The higher viscosity of the monomer-swollen polymer particles in the

64

Korea Polym. J., Vol. 9, No. 1, 2001

semicontinuous process, which is controlled by the rate of monomer addition, acts to reduce the contraction of the polymer shell and leads to the formation of composite particles, each of which has several lumps on their surface.

The thermodynamic analysis of the present polymerization system predicted the formation of such nonspherical particles from the combined effects of the interfacial free energies and the phase separation of the two polymer phases.

The effects of the monomer/polymer ratio and the nonionic surfactant dissolved in the monomer phase on the particle morphology were not enough to give the core-shell particles. The addition of grafting sites (double bonds) to the surface of seed particles improved the interfacial adhesion but not enough to give complete encapsulation of the carboxylated polystyrene core by the polystyrene shell. The most important factor which works against this encapsulation is the viscosity of the monomer-swollen polymer particles.

A hypothetical pathway based on the concept of opposing driving and resistance forces was proposed to prepare hydrophilic core/hydrophobic shell composite latex particles and confirmed by experimental evidence.

References

(1) R. Y. Dickie, M. F. Cheung, and S. Newman, *J. Appl. Polym. Sci.*, **17**, 65 (1973).

(2) D. I. Lee and T. Ishikawa, *J. Polym. Sci., Polym. Chem. Ed.*, **21**, 147 (1983).

(3) T. Min, A. Klein, M. S. El-Aasser, and J. W. Vanderhoff, *J. Polym. Sci., Polym. Chem. Ed.*, **21**, 2845 (1983).

(4) M. Okubo, *Makromol. Chem. Macromol. Symp.*, **35/36**, 307 (1990).

(5) I. Cho and K. Lee, *J. Appl. Polym. Sci.*, **30**, 1903 (1985).

(6) A. Bordon, *British Patent* 1,009,486 (1965).

(7) A. Bordon, *U.S. Patent* 3,291,768 (1966).

(8) A. Zosel and G. Ley, *Macromolecules*, **26**, 2222 (1993).

(9) K. M. Oconnor and S. L. Tsaur, *J. Appl. Polym. Sci.*, **33**, 2007 (1987).

(10) J. Richard, C. Mignaud, and K. Wong, *Polym. Int.*, **33**, 4164 (1992).

(11) V. I. Eliseeva, in *Emulsion Polymerization*, I. Piirma, Ed., Academic Press, 1982, pp 281.

(12) S. Muroi, H. Hashimoto, and K. Hosoi, *J. Polym. Sci., Polym. Chem. Ed.*, **22**, 1365 (1984).

(13) W. D. Ross, *J. Paint Tech.*, **43** (563), 50 (1971).

(14) A. Seiner and Gehart, *Ind. Eng. Chem. Prod. Res. Dev.*, **12** (2), 98 (1971).

(15) P. E. Pierce, S. Babil, and J. Blasko, *ACS, Div. Org. Coat. Plast. Chem.*, **33** (2), 271 (1973).

(16) S. Fitzwater and J. W. Hook III, *J. Coatings Tech.*, **57** (721), 39 (1985).

(17) J. L. Lando and H. T. Oakley, *J. Colloid Interface Sci.*, **25**, 526 (1967).

(18) K. Greene, *J. Colloid Interface Sci.*, **43**, 449 (1973).

(19) F. V. Loncar, Ph. D. Thesis, Lehigh University, 1985.

(20) W. Obrecht and W. Funke, *Makromol. Chem.*, **177**, 1877 (1976).

(21) J. Kim, Ph. D. Thesis, Lehigh University, 1986, pp. 46.

(22) J. Hearn, M. C. Wilkinson, and A. R. Goodall, *Adv. Colloid Interface Sci.*, **14**, 173 (1981).

(23) S. Yamazaki, *Kobunshi Ronbunshu*, **33**, 655 (1976).

(24) V. Dimonie, M. S. El-Aasser, A. Klein, and J. W. Vanderhoff, *J. Polym. Sci., Polym. Chem. Ed.*, **22**, 2197 (1984).

(25) S. Torza and S. G. Mason, *J. Colloid Interface Sci.*, **33**, 67 (1970).

(26) D. Sundberg, in *Advances in Emulsion Polymerization and Latex Technology*, 19th Annual short Course, June 6-10, 1988, Lehigh University.

(27) M. Okubo, Y. Katsuta, and T. Matsumoto, *J. Polym. Sci., Polym. Chem. Ed.*, **20**, 45 (1982).

(28) M. Okubo, A. Yamada, and T. Masumoto, *J. Polym. Sci., Polym. Chem. Ed.*, **18**, 3219 (1980).

(29) M. Okubo, M. Ando, A. Yamada, Y. Katsuta, and T. Matsumoto, *J. Polym. Sci., Polym. Letter Ed.*, **19**, 143 (1981).

(30) M. Chainey, M. C. Wilkinson, and J. Hearn, *Ind. Eng. Chem. Prod. Res. Dev.*, **21**, 171 (1982).

(31) J. M. Park, *J. Ind. Eng. Chem. (Korea)*, sumitted (2000).